

Cognition and Behavior

Theta-Phase Connectivity between Medial Prefrontal and Posterior Areas Underlies Novel Instructions Implementation

 **Silvia Formica**,^{1,2} **Carlos González-García**,^{2,3} **Mehdi Senoussi**,²  **Daniele Marinazzo**,⁴ and **Marcel Brass**^{1,2}

<https://doi.org/10.1523/ENEURO.0225-22.2022>

¹Berlin School of Mind and Brain, Department of Psychology, Humboldt Universität zu Berlin, Berlin 10117, Germany, ²Department of Experimental Psychology, Ghent University, Gent 9000, Belgium, ³Mind, Brain and Behavior Research Center, Department of Experimental Psychology, University of Granada, Granada 18071, Spain, and ⁴Department of Data Analysis, Ghent University, Gent 9000, Belgium

Abstract

Implementing novel instructions is a complex and uniquely human cognitive ability, which requires the rapid and flexible conversion of symbolic content into a format that enables the execution of the instructed behavior. Preparing to implement novel instructions, as opposed to their mere maintenance, involves the activation of the instructed motor plans, and the binding of the action information to the specific context in which this should be executed. Recent evidence and prominent computational models suggest that this efficient configuration of the system might involve a central role of frontal theta oscillations in establishing top-down long-range synchronization between distant and task-relevant brain areas. In the present EEG study (human subjects, 30 females, 4 males), we demonstrate that proactively preparing for the implementation of novel instructions, as opposed to their maintenance, involves a strengthened degree of connectivity in the theta frequency range between medial prefrontal and motor/visual areas. Moreover, we replicated previous results showing oscillatory features associated specifically with implementation demands, and extended on them demonstrating the role of theta oscillations in mediating the effect of task demands on behavioral performance. Taken together, these findings support our hypothesis that the modulation of connectivity patterns between frontal and task-relevant posterior brain areas is a core factor in the emergence of a behavior-guiding format from novel instructions.

Key words: cognitive control; connectivity; EEG; instructions following; phase-locking value; theta oscillations

Significance Statement

Everyday life requires the use and manipulation of currently available information to guide behavior and reach specific goals. In the present study we investigate how the same instructed content elicits different neural activity depending on the task being performed. Crucially, connectivity between medial prefrontal cortex (mPFC) and posterior brain areas is strengthened when novel instructions have to be implemented, rather than simply maintained. This finding suggests that theta oscillations play a role in setting up a dynamic and flexible network of task-relevant regions optimized for the execution of the instructed behavior.

Introduction

The ability to rapidly adapt to changing external contingencies is a crucial hallmark of human cognition. This

flexibility finds one of its most advanced and astonishing forms of expression in instructions following. Humans can

Received June 8, 2022; accepted June 23, 2022; First published July 22, 2022.
The authors declare no competing financial interests.

Author contributions: S.F., C.G.-G., M.S., D.M., and M.B. designed research; S.F. performed research; S.F. analyzed data; S.F., C.G.-G., M.S., D.M., and M.B. wrote the paper.

implement novel behaviors based on symbolic instructions, even in the absence of prior practice (Cole et al., 2013). For instance, the driver reaching unexpected roadworks might be presented with different options on how to proceed. They will have to encode and understand their content and execute one of them at the appropriate moment (e.g., “To reach the train station, take the second exit at the roundabout”). This apparently simple operation involves many complex cognitive processes, ultimately resulting in the execution of the correct behavior.

It is established that maintaining task information is not sufficient to successfully perform the instructed behavior (Milner, 1963; Duncan et al., 1996; Bhandari and Duncan, 2014). Rather, the abstract content of the instruction needs to be reformatted into an action-oriented code capable of driving behavior (Brass et al., 2017). At the hemodynamic level, several fMRI studies revealed a set of frontoparietal regions recruited to support novel stimulus-response mappings (SRs) implementation (Ruge and Wolfensteller, 2010; Demanet et al., 2016) and showing representational patterns specific to execution task demands (González-García et al., 2017; Muhle-Karbe et al., 2017; Bourguignon et al., 2018; Palenciano et al., 2019a). However, although evidence is accumulating concerning the neural substrate deployed for these reformatting purposes, the mechanisms binding stimulus and response information in an action-oriented format, and its exact nature, remain elusive.

In a recent EEG study, we investigated the differences in oscillatory activity associated with maintenance and implementation of novel instructions (Formica et al., 2021). The two tasks showed analogous attentional prioritization mechanisms, reflected in suppression of alpha power contralateral to the attended location (Jensen and Mazaheri, 2010; Gould et al., 2011; Bonnefond and Jensen, 2012; Myers et al., 2015; Mok et al., 2016). On the contrary, proactively transforming the content of the mapping into an action-oriented representation (i.e., the implementation task) elicited task-specific cognitive processes. Namely, preparing a defined motor plan was associated with stronger engagement of motor areas,

indexed by beta suppression over motor and premotor cortices (Cheyne, 2013; Schneider et al., 2017). Furthermore, increased theta power over midfrontal scalp electrodes during implementation was interpreted as a marker of working memory (WM) manipulation (Onton et al., 2005; Itthipuripat et al., 2013) and top-down control over alternative task sets (Miller and Cohen, 2001; Sauseng et al., 2010). Altogether, these findings represent crucial first insights into oscillatory mechanisms that are in place during the handling of novel task sets and nicely complement the existing fMRI literature. However, the fundamental question remains how binding between stimulus and response-related areas is achieved through oscillatory mechanisms.

Notably, midfrontal theta oscillations received increased attention in recent years because of their occurrence across a variety of tasks characterized by the need for cognitive control (Cohen and Donner, 2013; Cavanagh and Frank, 2014). Theories and evidence emerged regarding slow oscillations as prime mechanism for establishing top-down neural communication and for efficiently setting up functional networks optimized to meet task demands (Sauseng and Klimesch, 2008; McLelland and VanRullen, 2016; Voloh and Womelsdorf, 2016; Bonnefond et al., 2017; Riddle et al., 2020a,b). In line with this framework, recent computational models have attributed to theta oscillations a crucial role in flexibly binding posterior task-relevant areas (Verguts, 2017; Verbeke et al., 2020; Senoussi et al., 2022). Burst of theta-locked activity originating in the medial prefrontal cortex (mPFC) are directed toward the appropriate processing units (i.e., areas encoding task-relevant information), inducing the synchronization of their firing patterns and thus enabling efficient interareal communication (Fries, 2005, 2015). Crucially, the specific role of theta oscillations in instructions implementation remains untested.

Here, we set out to investigate the hypothesis that differences in medial prefrontal theta oscillations across task demands (i.e., maintaining vs implementing novel SRs) reflect the need to orchestrate the synchronization between posterior areas encoding stimulus and response information. We propose that the formation of a flexible network of task-relevant brain regions by means of long-range connectivity underlies the emergence of action-oriented representations, specifically involved in the implementation of novel instructions.

Materials and Methods

Participants

Thirty-five participants were recruited from the experimental pool of Ghent University and gave their informed consent at the beginning of the experiment, in accordance with the ethical protocols of Ghent University. Eligibility criteria included age between 18 and 35 years and no history of psychological or neurologic conditions. Sample size was not computed a-priori, but chosen to replicate the results of a previous study with a similar paradigm (Formica et al., 2021) and in line with the literature

This work was supported by Special Research Fund of Ghent University BOF.GOA.2017.0002.03 and the Deutsche Forschungsgemeinschaft (DFG, German Research Foundation) under Germany's Excellence Strategy, EXC 2002/1 “Science of Intelligence,” Project Number 390523135. C.G.-G. was additionally supported by the European Union's Horizon 2020 Research and Innovation Programme under the Marie Skłodowska-Curie Grant Agreement no. 835767 and the Spanish Ministry of Science and Innovation Grant ID IJC2019-040208-I. M.S. was supported by the Research Foundation Flanders (FWO) Grant Number G012816N and the Research Council of Ghent University Grant BOF17-GOA-004. M.B. is supported by an Einstein Strategic Professorship (Einstein Foundation Berlin).

Acknowledgments: We thank Dr. Ricardo Bruña and Dr. Emiel Cracco for the fruitful discussions, insightful comments, and kind support during data analysis.

Correspondence should be addressed to Silvia Formica at silvia.formica@hu-berlin.de.

<https://doi.org/10.1523/ENEURO.0225-22.2022>

Copyright © 2022 Formica et al.

This is an open-access article distributed under the terms of the [Creative Commons Attribution 4.0 International license](https://creativecommons.org/licenses/by/4.0/), which permits unrestricted use, distribution and reproduction in any medium provided that the original work is properly attributed.

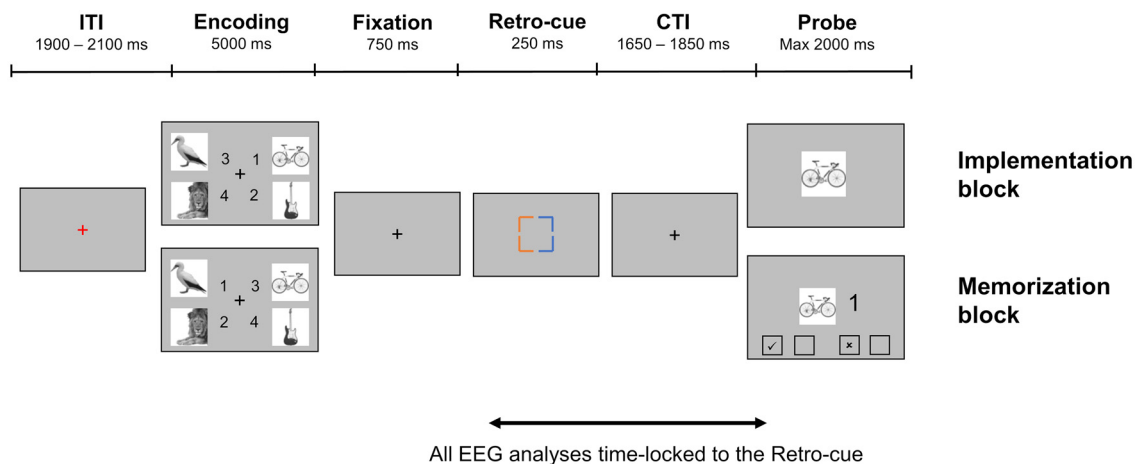


Figure 1. Task paradigm. ITI: inter-trial interval, CTI: cue-target interval.

on similar constructs (Schneider et al., 2017; de Vries et al., 2018; van Ede et al., 2019). The experiment consisted of two separate sessions, 1 to 3 days apart from each other. In the initial behavioral screening session (~30 min) participants practiced the two tasks, starting always with the Implementation task followed by the Memorization task. Initially, they could familiarize with the task requirements by performing without time pressure (i.e., no response deadline). After responding correctly to five consecutive trials, the normal 2000 ms response deadline was introduced. Participants then completed four mini blocks of 15 trials each, receiving feedback after each response and at the end of the block as percentage of accurate responses. If overall performance in the 60 trials reached an accuracy threshold of 70% in both tasks, the participant was invited to take part in the EEG session, otherwise they would be compensated for the behavioral screening (5 €). Participants could repeat the practice blocks once if they did not reach the threshold at their first attempt. Two participants repeated the practice for the Memorization task, and one participant for the Implementation task. Eventually, all participants reached the required threshold in both tasks. One participant dropped out after completing the behavioral screening, leaving a sample of 34 participants in the main EEG session ($M_{Age} = 21.73$, $SD_{Age} = 3.29$, 30 females, four males). All participants had normal or corrected-to-normal vision and 29 reported to be right-handed. Data from three participants were discarded because of low task performance (their individual accuracy exceeded by 2.5 SD the mean group accuracy and/or their accuracy was below 60% in response to catch trials in at least one of the two tasks). One additional participant was discarded because of noisy EEG recordings. Therefore, our final sample consisted of 30 participants.

Materials

The set of stimuli consists of three macrocategories: animate (nonhuman animals), inanimate 1 (vehicles and musical instruments), inanimate 2 (household tools and

clothes), each with approximately 700 items (Griffin et al., 2007; Konkle et al., 2010; Brady et al., 2013; Brodeur et al., 2014; González-García et al., 2020). All pictures were centered in a 200×200 pixels canvas, were converted to grayscale, and had their background removed.

Procedure

Stimuli presentation and response collection were performed using the Psychopy toolbox (Peirce, 2007). In the EEG session, participants performed both tasks (i.e., Implementation task and Memorization task), in a blocked design, with task order counter-balanced across participants. Trial structure was identical in the two tasks, except for the probe screen (Fig. 1). Each trial started with a red fixation cross presented in the middle of the screen for 2000 ms (± 100 ms), indicating the intertrial interval. Next, four SRs were presented simultaneously for 5000 ms, one for each quadrant of the screen. Each mapping consisted of one image and one digit from 1 to 4, corresponding to the four response options (1: left middle finger, key “e”; 2: left index finger, key “r”; 3: right index finger, key “i”; 4: right middle finger, key “o”). Importantly, responses could be organized according to two response schemes. Namely, mappings involving a response with the left(right) hand could be presented on the left(right) side of the encoding screen; or they could be presented on the right(left) side of the encoding screen, the latter case resulting in an incongruency between location on the screen and response hand. This was done to orthogonalize the presentation side on the encoding screen and the required response hand. To simplify the encoding of the four mappings, index fingers responses were always associated with the two upper images, and middle fingers responses with the lower images. Each encoding screen contained two images from two different categories, grouped on the left and right side of the screen. Each image was presented only once throughout the whole experiment to ensure the novelty of all mappings. After the presentation of the mappings, a fixation interval of 750 ms was presented, considered sufficiently long to

prevent iconic memory traces (Souza and Oberauer, 2016), followed by a retro-cue presented centrally for 250 ms. The retro-cue consisted of four colored corners, pointing to the four quadrants previously occupied by the mappings. Each side of the retro-cue was colored in either blue (RGB = [0, 155, 255]) or orange (RGB = [255, 100, 0]). These colors were chosen to equate luminance and saliency, thereby preventing low-level confounds imputable to exogenous attention. Participants were instructed at the beginning of the experiment that one color indicated the two mappings relevant for the task, and the other color pointed to the location of mappings that could be discarded. Color assignment was counter-balanced across participants and remained the same for the whole duration of the experiment. The information provided by this retro-cue allowed participants to select two out of the four initially encoded mappings. The selected mappings always contained images belonging to the same category and involved responses with the index and middle fingers of the same hand. In the example trial presented in Figure 1, assuming the relevant color was blue, the participant would have had to retain the two mappings presented on the right side of the screen and containing the two inanimate images, namely bicycle and guitar. The unselected animate images (i.e., bird and lion) could be dropped from WM. The retro-cue was followed by a cue-target interval (CTI) with a jittered duration of 1750 ms (± 100 ms). Next, the probe appeared and remained on screen for a maximum duration of 2000 ms or until button press. If no response was provided within the response deadline, a message appeared encouraging the participant to take a short break if needed, and to press the spacebar to resume the task. In the Implementation task, the target consisted of a choice-reaction task, with one of the selected images presented centrally. In the example, either the bicycle or the guitar could appear. Participants were asked to press the key with the finger associated to the corresponding mapping. The Memorization task was a delayed match-to-sample task, in which participants were presented centrally with one of the selected images and a response digit. This target mapping had to be compared with the encoded ones, to verify whether the image-response association was correct. Participants provided their response by pressing with the finger corresponding to the tick sign (\checkmark) or \times sign (\times) displayed at the bottom of the probe screen, to indicate matching or mismatching mappings, respectively. Notably, the assignment of \checkmark and \times locations with respect to the four fingers was randomized on each trial. This task design ensured that the two tasks differed only to the extent a specific response could be proactively prepared during the CTI. In the Implementation task, participants were encouraged to prepare the SRs for execution as soon as the retro-cue indicated the relevant two. On the contrary, the Memorization task only allowed for a declarative maintenance of the two selected mappings, because no action-oriented representation could be built and thus no action plan prepared.

In both tasks, 10% of trials featured a completely new image as target, instead of one of the encoded (i.e., catch trials). Participants were instructed to press the spacebar in such events. This was done to ensure all four mappings were initially encoded, discouraging strategies such as focusing only on a subset of mappings. Since we were interested in the brain activity during the CTI, catch trials were included in our analyses.

During the EEG session, 240 trials for each task were completed, divided in six blocks. Trials were equally distributed between the four conditions resulting from the characteristics of the selected mapping, namely the side they appeared on in the encoding screen (Cued Side, left or right) and the response hand they involved (Response Side, left or right). Therefore, the task used in the current study differed from our previous design (Formica et al., 2021) insofar it capitalized on lateralized stimuli presentation and response preparation.

Experimental design and behavioral analysis

The study consisted of three within-subject factors orthogonally manipulated. Namely, Task (Implementation vs Memorization), Cued Side (left vs right) referring to the location on the screen of the selected mappings, and Response Side (left vs right), indicating the response hand involved in the selected mappings. Based on previous studies comparing implementation and maintenance of novel SRs, we expected to find shorter reaction times (RTs) and lower error rates for the former with respect to the latter (Demant et al., 2016; Formica et al., 2020, 2021; González-García et al., 2020). Therefore, we used JASP (JASP Team, 2019) to compare RTs and error rates across Tasks, separately for regular and catch trials. RTs were analyzed by means of paired-samples *t* tests. Error rates distributions for both regular and catch trials violated the normality assumption (Shapiro–Wilk test $p < 0.05$), and thus the results of Wilcoxon signed-rank tests are reported.

EEG recordings and preprocessing

Electrophysiological data were collected using a BioSemi ActiveTwo system (BioSemi) with 64 Ag–AgCl electrodes arranged in the standard international 10–20 electrode mapping (Klem et al., 1999), with a CMS-DRL electrode pair. Two external electrodes were placed on the left and right mastoid for online referencing. Four additional external electrodes (two to the outer canthi of both eyes, one above and one below the left eye) were used to monitor horizontal and vertical eye movements. Data were recorded at a sampling rate of 1024 Hz.

All preprocessing and analyses steps were conducted with the Python MNE toolbox version 0.22.0 (Gramfort, 2013). First, a 1- to 40-Hz bandpass FIR filter was applied to the continuous data (Hamming window with 0.0194 passband ripple and 53-dB stopband attenuation, with lower and upper transition bandwidth of 1 and 10 Hz, respectively). Next, data were epoched time-locked to the onset of the retro-cue (from -1000 to 2500 ms),

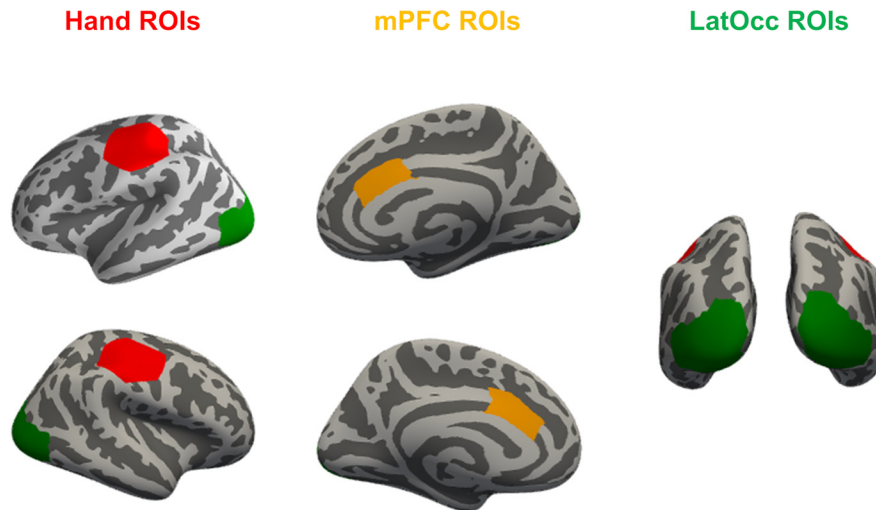


Figure 2. ROIs locations. mPFC and LatOcc ROIs were obtained from the Desikan–Killiany atlas (caudal anterior cingulate and lateral occipital parcels, respectively). Hand ROIs were drawn with a 30-mm radius around the MNI motor areas hand coordinates ($[\pm 44, -17, 49]$).

demeaned to the average of the whole time window to improve independent component analysis (ICA; Groppe et al., 2009), and downsampled to 512 Hz. Trials containing excessive muscle activity or other clear artifacts were rejected based on visual inspection, and electrodes showing noise for a large portion of epochs were removed and interpolated using the spherical spline method (Perrin et al., 1989). Data were then re-referenced to the average of all channels. Finally, eye movements were removed by means of ICA: an average of 2.23 (SD = 0.716) ICA components were removed for each participant.

Only trials with a correct response were retained for the analyses. This resulted in an average of 218.23 trials for Implementation (SD = 18.89) and 212.70 for Memorization (SD = 12.02). For each individual condition (e.g., SRs presented on the left side of the screen and requiring a left-hand response), an average of 53.86 trials (SD = 4.55) were retained (range 36–60 across participants).

Source reconstruction

To project brain activity from the sensors to the source space, we employed the default anatomic template included in the MNE-Python toolbox ('fsaverage' from FreeSurfer) and decimated the dipole grid on the white matter surface to 4098 sources per hemisphere (sixth grade subdivisions of an octahedron). A realistic Boundary Element Model (BEM) was created assuming specific conductivity for each of the three shells (skin, outer and inner skull). Noise in the recordings was estimated by computing a noise covariance matrix from the baseline period (−500 to −200 ms) and the inverse problem was then solved with the dynamic statistical parametric mapping (dSPM) method (Dale et al., 2000).

Regions of interest (ROIs) definition

We focused our analyses on an a-priori set of ROIs. From the Desikan–Killiany atlas (Desikan et al., 2006), we

obtained left and right lateral occipital parcels (LatOcc ROIs), and left and right caudal anterior cingulate parcels (mPFC ROIs), an area that showed to be consistently activated across a variety of processes for cognitive and adaptive control (Cavanagh and Shackman, 2015; De La Vega et al., 2016). Additionally, we created Hand ROIs by grouping sources within a radius of 30 mm on the inflated surface from the MNI coordinates for the left and right hands ($[\pm 44, -17, 49]$; Zhao et al., 2019). The resulting set of ROIs is depicted in Figure 2.

Statistical approach

To evaluate the statistical significance of the differences between time courses in our contrasts of interest, we adopted a cluster-based permutation approach (Maris and Oostenveld, 2007). Importantly, this method is effective in evaluating the reliability of neural data patterns over contiguous timepoints, while successfully controlling for the multiple comparisons problem. First, the time courses are compared with an F test (or t test, depending on the specific contrast) between all timepoints of the observed conditions, with an α level of 0.05. Next, neighboring time points with above threshold same sign significance are grouped together, and the resulting segment of data are considered a cluster with a size corresponding to the sum of the F values (or t values) of all time points belonging to it. The statistical significance of these observed clusters is computed by comparing them to a distribution of clusters obtained under the null hypothesis. Specifically, surrogate data are generated for 10,000 permutations by randomly flipping the sign of the difference between conditions. A distribution of cluster sizes under the null hypothesis of no differences between conditions is obtained by taking the size of the largest cluster (computed as for the observed data) for each of the permutations. The P-value for each observed cluster corresponds to the proportion of permutations in which a cluster larger than the observed one was found. Again, we used an α level of 0.05, therefore

retaining as significant only clusters larger in size than at least 95% of clusters in the surrogate data. It is important to point out that because of the nature of the second-level inference between observed and surrogate distributions, the exact boundaries of each cluster (i.e., first and last time points) have to be interpreted cautiously and do not reflect the significance of each individual time point (Sassenhagen and Draschkow, 2019).

For each observed cluster, an average effect size is computed as Cohen's *d*. To obtain it, the difference between the two conditions in the mean values over the time window of significance of the cluster is derived, and then divided by its SD.

All statistical analyses are performed in the time window 0–1800 ms from retro-cue onset. The CTI was jittered, with a duration between retro-cue onset and probe onset ranging between 1900 and 2100 ms. Therefore, the time window for analyses was cut 100 ms before the earliest probe onset, to reduce the influence of the smearing in time resulting from the time-frequency analysis linked to the processing of the probe.

Spectral analysis

For each condition, the induced power was computed in the source space for three frequency ranges (theta: 3–7 Hz, alpha: 8–14 Hz, beta: 15–30 Hz). Time-frequency decomposition was performed by means of complex Morlet wavelets, in steps of 1 Hz and with the number of cycles adapted to the frequency range (three cycles for theta, four cycles for alpha, and five cycles for beta), to achieve a good trade-off between temporal and frequency precision (Cohen, 2014). The resulting decomposed data were then averaged within each frequency range and further downsampled to 128 Hz.

Attentional contralateral alpha suppression

When orienting attention to the external or internal space, a suppression of alpha power has been traditionally observed over posterior areas contralateral to the attended hemisphere (Jensen and Mazaheri, 2010; Gould et al., 2011; Bonnefond and Jensen, 2012; Myers et al., 2015; Mok et al., 2016). For each condition, time courses of alpha (8–14 Hz) power for the left and right LatOcc ROIs were obtained by taking the first right-singular vector of the single value decomposition of all sources within the ROI, scaled to their average power and adjusted in sign for the orientation of each single dipole ('pca_flip' method). In other words, this procedure results in a time course explaining the largest possible amount of variance in the whole ROI. The time courses were then collapsed across conditions to obtain an ipsilateral and a contralateral time course with respect to the Cued Side, separately for each of the two tasks. According to our hypotheses and previous findings (Formica et al., 2021), we expected to observe significant alpha suppression in the contralateral hemisphere, and no differences between Tasks. To test for this hypothesis, we performed a repeated-measures ANOVA (rmANOVA) with factors Tasks (Implementation vs Memorization)

and Laterality (ipsilateral vs contralateral with respect to the selected hemisphere), adopting a cluster-based permutation approach as described below (Statistical analysis).

Motor contralateral beta suppression

Similarly, beta power is suppressed over the motor cortex contralateral to the limb being prepared for movement (Cheyne, 2013). Time courses of beta (15–30 Hz) power activity were extracted from the Hand ROIs ipsilateral and contralateral to the response hand required by the selected mappings, with a procedure analogous to the one used for alpha. Here, we predicted a larger contralateral suppression in Implementation compared with Memorization, because of the proactive preparation of the specific motor plan instructed by the mapping. Therefore, we performed an rmANOVA with factors Tasks (Implementation vs Memorization) and Response Side (contralateral vs ipsilateral to the instructed response hand).

Task-specific theta increase

Previous studies showed larger theta power during tasks requiring the exertion of cognitive control and the extensive manipulation of WM content (Onton et al., 2005; Cavanagh and Frank, 2014; Formica et al., 2021). According to prominent computational models, this phenomenon can be interpreted as reflecting the activity of the mPFC in coordinating the neural communication between distant task-relevant areas (Voloh and Womelsdorf, 2016; Verguts, 2017). Therefore, we extracted a time course of theta (3–7 Hz) power activity from the bilateral mPFC ROIs for each of the two Tasks, and we compared them, predicting larger values for Implementation.

Mediating effect of theta power on RTs

We further hypothesized mPFC theta oscillations to play a role in determining behavioral performance. Namely, we tested whether theta power mediates the effect of Task on RTs.

Trial-by-trial theta power was defined as the average theta (3–7 Hz) power in a time window of length 633 ms centered on the cluster of significant difference between Tasks (Materials and Methods, Task-specific theta increase). This resulted in an interval spanning from 355 to 985 after retro-cue onset. The choice of this duration is motivated by the need to encompass at least two oscillatory cycles at the lowest frequency of interest (3 Hz). Given that single-trial power estimation led to some outliers because of noisy trials, for each participant we removed trials in which the computed mean theta power exceeded 3 SDs from the individual mean. Analogously, RTs were trimmed, separately for each Task and participant, removing trials with latencies exceeding 3 SDs from the mean (importantly, similar results were obtained without applying any filtering procedure to the data). This trimming approach resulted in an average of 6.47 (± 2.11 , 1.68%) trials being removed because of outlier values of

theta power, $3.1 (\pm 1.3, 1.58\%)$ and $1.47 (\pm 1.63, 0.75\%)$ trials being removed with respect to RTs in the implementation and memorization task, respectively.

To empirically test the prediction that theta power mediates the effect of Task on RTs, we started by verifying the necessary criteria put forward by Baron and Kenny (1986). Namely, it had to be confirmed that Tasks influences both RTs and theta power, and that theta power predicts RTs. We fitted linear mixed effects models (LMMs) using the lme4 package in R (Bates et al., 2014), adopting a backward selection approach to define the random effect structure of the model (Matuschek et al., 2017). The reported P-values were calculated using Satterthwaite approximations (Luke, 2017). Finally, to formally and directly test the mediation effect, a causal mediation analysis was performed with the mediation package in R (Tingley et al., 2014).

Functional connectivity: phase locking value (PLV)

According to the computational model proposed by Verguts (2017) and updated by his colleagues (Verbeke and Verguts, 2019; Verbeke et al., 2020; Senoussi et al., 2022), theta oscillations from the mPFC control unit serve the purpose of synchronizing posterior task-relevant processing units. Therefore, we were primarily interested in investigating whether task demands (i.e., preparing for Implementation vs Maintenance) affect connectivity between frontal and posterior areas.

To estimate phase synchronization between pairs of ROIs, we first bandpass filtered our epoched data in the theta frequency range (3–7 Hz; Hamming window with 0.0194 passband ripple and 53-dB stopband attenuation, with lower and upper transition bandwidth of 2 Hz). After projection to the source space, data were Hilbert transformed to obtain the analytic signal from which to extract the phase information. Then, we computed the PLV, a measure reflecting the instantaneous phase difference between two signals, with the assumption that two brain areas that are configured to communicate efficiently should have a constant phase difference (Lachaux et al., 1999; Mormann et al., 2000). Instead of extracting a representative time course for each ROI, resulting in loss of information, we adopted a recently proposed multivariate approach, that allows to efficiently estimate the PLV across all pairwise sources of the two ROIs (Bruña et al., 2018; Bruña and Pereda, 2021). Therefore, the connectivity estimate for each pair of ROIs was obtained by taking the root square value of the $M \times N$ matrix containing the pairwise PLV between all sources, where M is the number of sources in ROI 1 and N the number of sources in ROI 2.

PLV between pairs of ROIs was computed for each trial in the time window from 355 to 985 ms, resulting in a value of synchronization for each trial, participant, and ROIs pair of interest. It is worth pointing out that PLV is sensitive to volume conduction and source leakage, thus prone to identify spurious connectivity between two neighboring sensors or brain regions reflecting activity from the same source. This concern is moderated in the present study by the selection of ROIs relatively distant

from each other, and, most importantly, by comparing connectivity of pairs of ROIs between conditions (see below - section Functional connectivity between mPFC and motor and visual areas). Although the magnitude of PLV might theoretically be inflated by source leakage, our hypotheses are focused on how PLV between pairs of ROIs is influenced by different task demands, and therefore are unaffected by this potential issue.

Functional connectivity between mPFC and motor and visual areas

We expected the synchronization between frontal and motor areas to be stronger when preparing to implement the SRs, because of the activation and binding of the instructed motor plan. Additionally, we had a further corollary hypothesis, namely that differences between tasks were expected to be driven predominantly by an increase of synchronization between mPFC and the Hand ROI contralateral to the currently relevant response hand in Implementation, but not so in Memorization. In other words, we expected an interaction between the factors Task and Response Side (collapsed for contralateral vs ipsilateral), with a specific directionality. To this aim, we fitted an LMM estimating the trial-by-trial PLV value using Task and Laterality (contralateral vs ipsilateral) as predictors. The model fitting procedure was analogous to the one described above and was conducted using only correct regular trials. The selected model structure included Task, Laterality and their interaction as fixed effects, a random intercept for each participant and a random slope for Task [in lmer notation: $PLV(mPFC-Hand) \sim Task * Laterality + (1 + Task | Subject)$].

Similar hypotheses and analyses were proposed with respect to connectivity between mPFC and visual areas. The trial-by-trial PLV between mPFC and LatOcc ROIs was fitted with an LMM, predicting an interaction of the factors Task and Laterality (defined as ROI contralateral or ipsilateral to the Cued Side). Model structure was analogous to the one reported for the connectivity between mPFC and Hand ROIs [$PLV(mPFC-LatOcc) \sim Task * Laterality + (1 + Task | Subject)$].

Results

Behavioral results

Based on previous studies reporting performance on implementation and maintenance of novel SRs (Demagnet et al., 2016; Formica et al., 2020, 2021; González-García et al., 2021), we expected faster and more accurate responses in the Implementation compared with Memorization task. Indeed, a paired-samples t test on RTs of regular trials yielded a large effect of Task ($t_{(29,1)} = 29.101, p < 0.001$, Cohen's $d = 5.313$), with average RTs in the Implementation task (mean = 708 ± 129 ms) being shorter than in the Memorization task (mean = 1217 ± 123 ms). Similarly, a Wilcoxon signed-rank test on error rates showed significantly less errors ($W_{(29,1)} = 65.5, p = 0.003$, Effect size = 0.653) in Implementation (mean = 0.060 ± 0.047) compared with Memorization (mean = 0.089 ± 0.029).

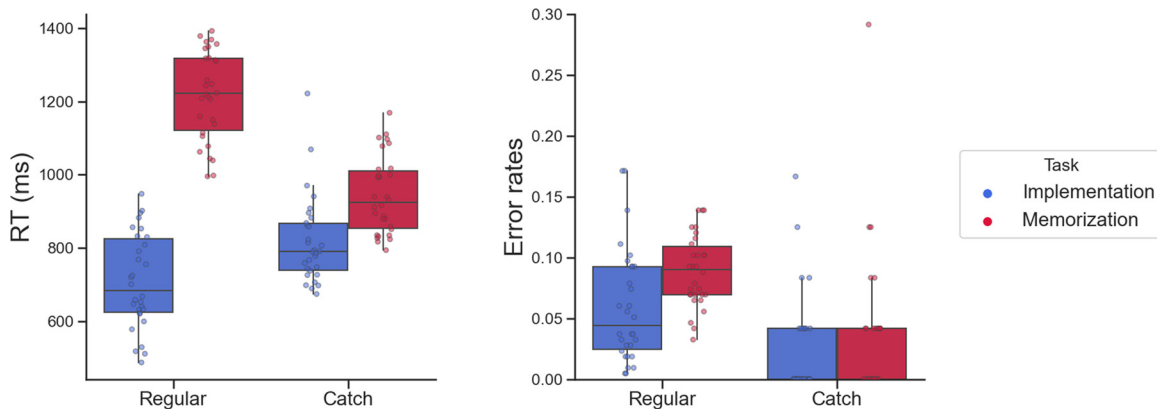


Figure 3. Behavioral results. Left panel, RTs (milliseconds). Right panel, Error rates. In each boxplot, the thick line inside box plots depicts the second quartile (median) of the distribution ($n=30$). The bounds of the boxes depict the first and third quartiles of the distribution. Whiskers denote the 1.5 interquartile range of the lower and upper quartile. Dots represent individual subjects' scores. Results for the 2 (Task) \times 2 (Cued Side) \times 2 (Response Side) rmANOVAs on RTs and error rates of regular trials are reported in Extended Data Figure 3-1.

RTs and accuracy were compared across Tasks also with respect to catch trials. A paired samples t test showed support ($t_{(29,1)} = 6.508$, $p < 0.001$, Cohen's $d = 1.188$) for faster RTs in response to catch trials in Implementation (mean = 817 ± 119 ms) compared with Memorization (mean = 943 ± 105 ms). On the contrary, no reliable difference ($W_{(29,1)} = 95.5$, $p = 1$, Effect size = 0.005) in their accuracy (Implementation: mean = 0.035 ± 0.070 ; Memorization: mean = 0.036 ± 0.061 ; Fig. 3).

Attentional contralateral alpha suppression

To test our hypothesis that posterior alpha power tracks the orienting of attention toward the selected hemifield analogously in the two tasks, we performed a rmANOVA on the power time courses we extracted from the LatOcc ROIs, with factors Tasks (Implementation vs Memorization) and Laterality (contralateral vs ipsilateral to the attended hemisphere). As predicted, we observed a strong reduction in alpha power contralateral to the attended hemisphere (main effect of Laterality, $p < 0.001$, cluster corrected, $d = 1.37$). Importantly, no cluster of differences emerged when contrasting the two Tasks, nor when testing for the interaction of the two factors (Fig. 4).

Motor contralateral beta suppression

Activation of a specific motor plan is a crucial component of the preparation to implement novel SRs. This will then be reactivated in a reflex-like manner upon stimulus presentation (Liefoghe et al., 2012). In line with this assumption, we expected beta suppression over motor cortices to clearly track the response hand involved in the selected mappings, and particularly in the Implementation task. In other words, we predicted the time courses of beta power from the Hand ROIs to show a significant interaction in a rmANOVA with factors Tasks (Implementation vs Memorization) and Laterality (contralateral vs ipsilateral to the instructed response hand). We found a large significant cluster for the main effect of Laterality ($p = 0.002$, cluster corrected, $d = 0.69$). Additionally, we tested for

the directional effect of the interaction with a one-sided t test (i.e., Implementation $<$ Memorization), and obtain a cluster with $p = 0.077$ ($d = 0.49$). No cluster was found when testing for the main effect of Task (Fig. 5).

Task-specific theta increase

We predicted Implementation and Memorization to differ with respect to theta oscillations in the mPFC. Specifically, we used cluster-based permutation to test for larger mPFC theta power amplitude in Implementation compared with Memorization. We observed a significant cluster ($p = 0.035$, cluster corrected, $d = 0.57$; Fig. 6). Additionally, we confirmed the spatial specificity of this effect by showing no differences in theta oscillations in Hand and LatOcc ROIs.

Activity in the medial wall of the PFC and oscillations in the theta frequency range have been both associated with handling conflict (Cavanagh and Frank, 2014; Cavanagh and Shackman, 2015). To rule out the possibility that mPFC activity reflects the conflict elicited by incongruent conditions (i.e., trials in which the retro-cue instructed participants to orient attention toward SRs on one side of the screen and to prepare responding with the opposite hand; as compared with trials with same Cued and Response Side), that could be larger specifically in the Implementation task, we performed additional control analyses. Namely, we compared differences in theta in congruent and incongruent trials, separately for Implementation (no clusters observed), Memorization ($p = 0.168$, cluster-corrected, $d = 0.46$), and across tasks (no clusters observed). Moreover, the effect of Congruency did not differ between the two Tasks (no clusters observed). Additionally, we tested for the effect of Task separately for congruent and incongruent trials. While there was a significant difference between Tasks in congruent trials ($p = 0.033$, cluster-corrected, $d = 0.54$), this was not the case for incongruent trials ($p = 0.124$, cluster-corrected, $d = 0.43$). Although these results cannot be taken as evidence for an interaction between the factors Task and

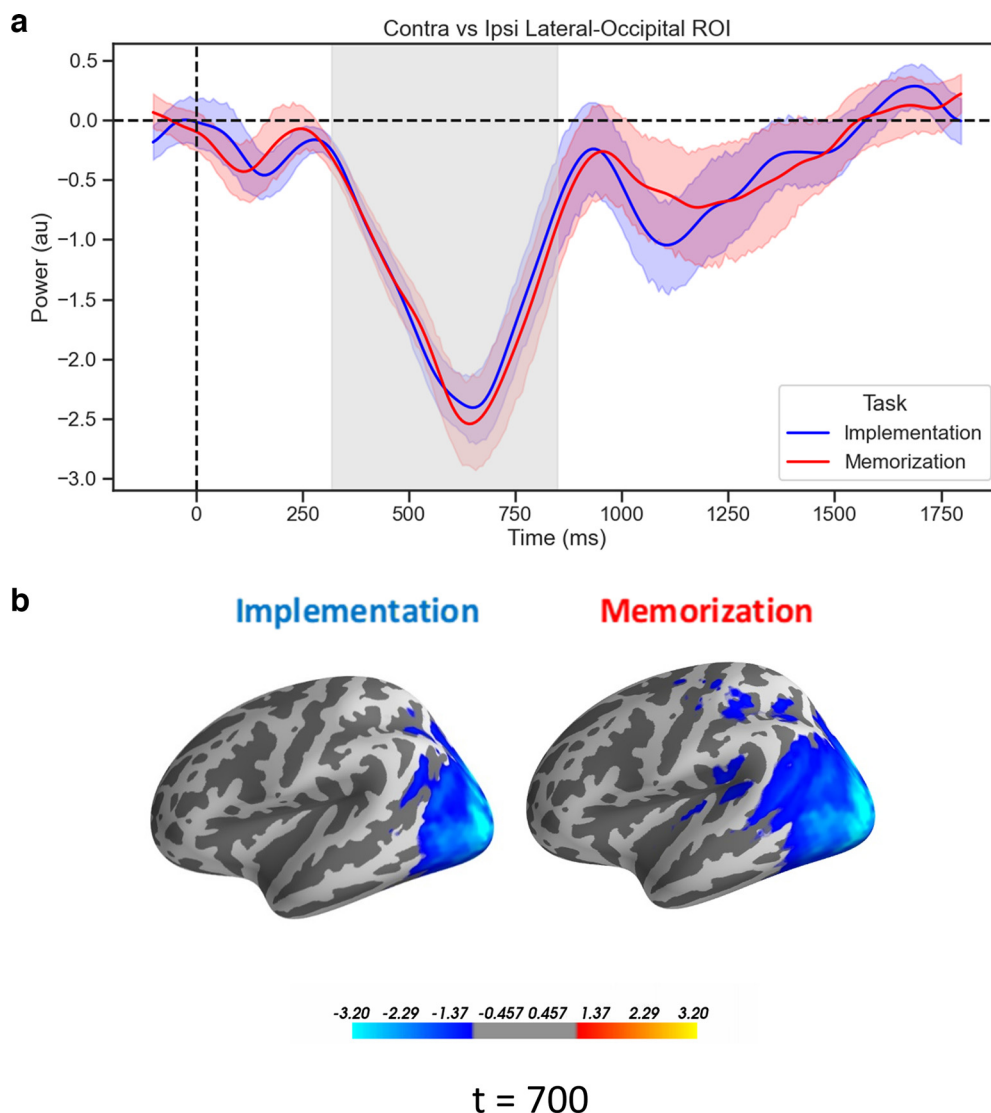


Figure 4. Attentional contralateral alpha suppression. **a**, Time courses of the difference waves (contralateral vs ipsilateral) of α power from the LatOcc ROIs, time-locked to the onset of the retro-cue. Shading indicates the SEM, gray area refers to the extent of the significant cluster for the effect of Laterality ($p < 0.001$, cluster corrected). **b**, Source-reconstructed activity of the alpha power for the difference between contralateral and ipsilateral Cued Side, at 700 ms, for visualization purposes.

Congruency (Nieuwenhuis et al., 2011), they are hinting at a larger difference in theta oscillations between Tasks in congruent trials (i.e., trials eliciting less conflict). Taken together, these exploratory analyses support our interpretation that the observed mPFC activity is indicative of differences between Tasks rather than the by-product of conflict resolution.

mPFC theta power mediates the effect of task on RTs

We hypothesized that trial-by-trial theta power in the mPFC mediated the effect of Task on behavioral performance. First, we tested for an effect of Task on RTs, by fitting an LMM with a fixed effect of Task, a random slope for Task, and a random intercept for each participant [$RT \sim Task + (1 + Task | Subject)$]. As expected, Implementation was associated with significantly faster RTs ($t_{(28.83)} = -28.75$, $\beta = -257.50$, CI 95% = $[-275.05$,

$-239.94]$, $p < 0.001$). Moreover, by fitting an LMM with identical structure to predict theta power [$Mean_Theta \sim Task + (1 + Task | Subject)$], we showed that single-trial variations in mPFC theta power were significantly dependent on task demands ($t_{(28.83)} = 2.72$, $\beta = 0.10$, CI 95% = $[0.03, 0.18]$, $p = 0.011$), such that larger theta values were associated with the Implementation task.

Finally, we also tested for the fixed effects of both Task and theta power (while assuming random slope for Task and random intercept for each participant) by fitting the LMM $RT \sim Mean_theta + Task + (1 + Task | Subject)$. We found a significant effect of theta power $t_{(11200.23)} = -3.54$, $\beta = -3.29$, CI 95% = $[-5.11, -1.47]$, $p < 0.001$, suggesting faster RTs for larger theta values. The effect of Task was significant, $t_{(28.83)} = -28.70$, $\beta = -257.16$, CI 95% = $[-274.72, -239.60]$, $p < 0.001$. Note that adding an interaction term as fixed effect to this model (i.e.,

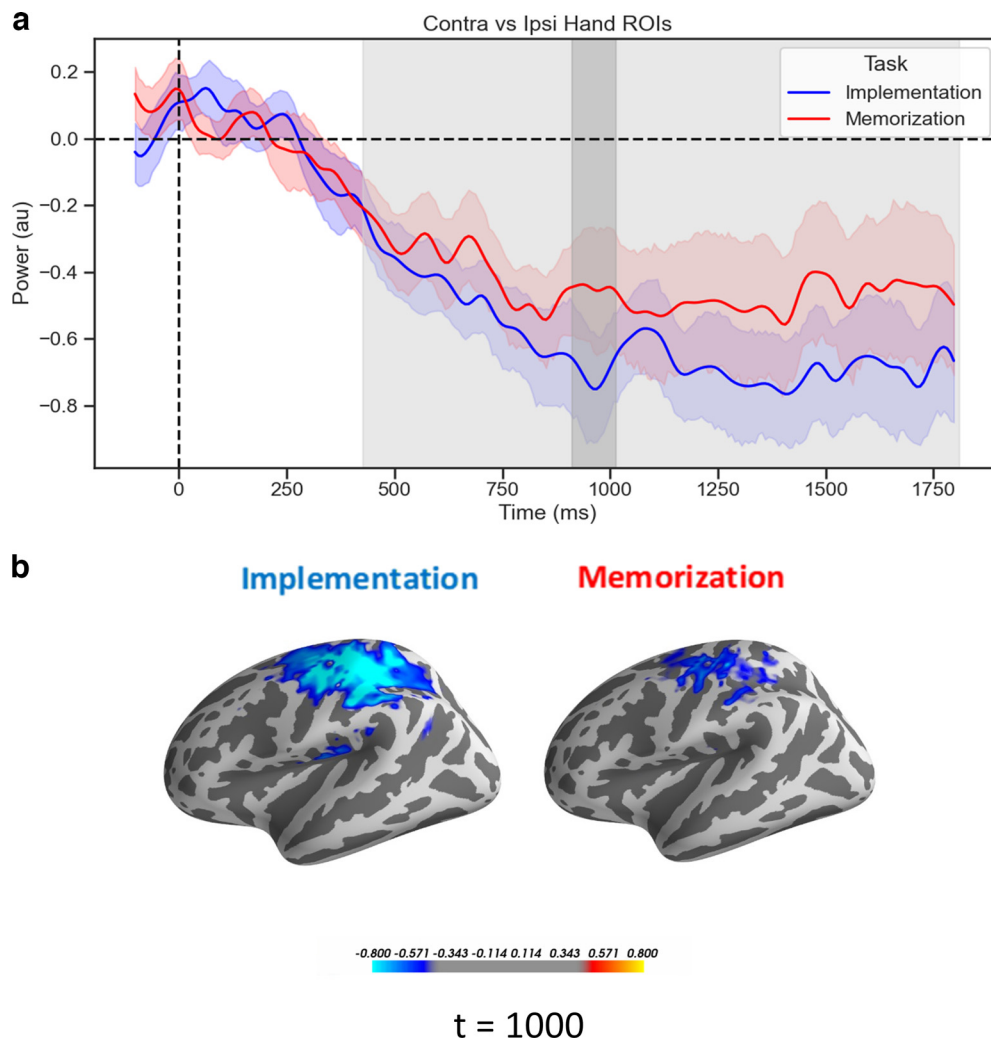


Figure 5. Motor contralateral beta suppression. **a**, Time courses of the difference waves (contralateral vs ipsilateral) of beta power from the Hand ROIs, time-locked to the onset of the retro-cue. Shading indicates the SEM, light gray area refers to the extent of the significant cluster for the effect of Laterality ($p = 0.002$, cluster corrected), dark gray area refers to the cluster for the interaction of Laterality and Task ($p = 0.077$, cluster corrected). **b**, Source-reconstructed activity of the beta power for the difference between contralateral and ipsilateral Response Side, at 1000 ms, for visualization purposes. au: arbitrary units.

Mean_Theta * Task) did not result in a significant interaction effect ($p = 0.66$; Fig. 7a).

This pattern of results suggests that theta partially mediated the effect of task, and this was directly tested by a causal mediation analysis revealing not only a significant direct effect of Task on RTs, $\beta = 514$, CI 95% = [477, 549.73], $p < 0.001$, but also a significant indirect effect via theta power, $\beta = 0.66$, CI 95% = [0.11, 1.42], $p = 0.013$, indicative of a partial mediation (Fig. 7b).

Functional connectivity between mPFC and motor/visual areas

To test our hypothesis that preparing to implement SRs is characterized by increased connectivity in theta band between frontal and motor areas, we used LMM to estimate whether different task demands resulted in different PLV values between mPFC and Hand ROIs. We fitted a model with a fixed effect for Task, Laterality and their

interaction, a random effect for Task and a random intercept for each participant [$PLV(mPFC-Hand) \sim Task * Laterality + (1 + Task | Subject)$]. We found a significant effect of Task ($t_{(0,29)} = 3.04$, $\beta = 0.008$, CI 95% = [0.0003, 0.001], $p = 0.005$), thus proving stronger connectivity during Implementation compared with Memorization (Fig. 8). Contrary to our hypothesis, the effect of Laterality and its interaction with Task were not significant ($p = 0.16$ and $p = 0.71$, respectively).

Analogously, we tested whether task demands affected the degree of connectivity between frontal and visual areas. We fitted a model with the structure $PLV(mPFC-LatOcc) \sim Task * Laterality + (1 + Task | Subject)$. We found a significant effect of Task ($t_{(0,29)} = 2.96$, $\beta = 0.008$, CI 95% = [0.0002, 0.001], $p = 0.006$), supporting our hypothesis of stronger connectivity during Implementation compared with Memorization (Fig. 8). Again, the effect of Laterality and the interaction of Laterality and Task were not significant ($p = 0.38$ and $p = 0.85$, respectively).

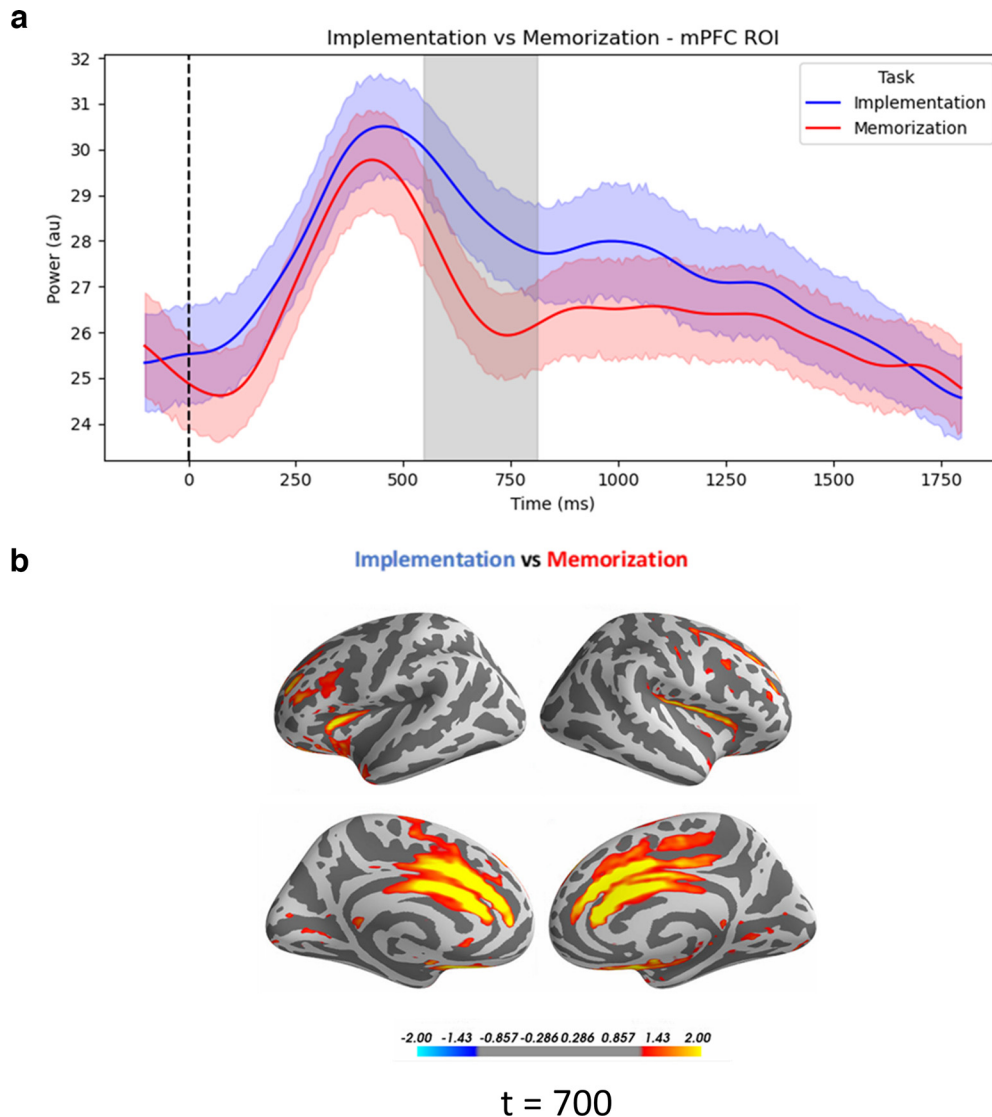


Figure 6. Task-specific theta increase. **a**, Time courses of theta power from the mPFC ROIs, time-locked to the onset of the retro-cue. Shading indicates the SEM, gray area refers to the extent of the significant cluster for the effect of Task ($p = 0.035$, cluster corrected). Time courses of theta power time-locked to the retro-cue from Hand and LatOcc ROIs are reported in Extended Data Figure 6-1. **b**, Source-reconstructed activity of theta power for the difference between Implementation and Memorization, at 700 ms, for visualization purposes. au: arbitrary units.

To confirm the spatial specificity of our main connectivity results and to test whether the observed PLV differences across Tasks could be because of field spread rather than genuine functional connectivity, we repeated the same analyses with control regions, namely left and right Parahippocampal ROIs from the Desikan–Killiany atlas. These areas were chosen because roughly equidistant from all three sets of ROIs used in our main analyses, and because we assumed they are not involved in performing the two tasks. We computed the PLV between mPFC and Parahippocampal ROIs using the same pipeline adopted for the main analyses. We found no main effect of Task ($F = 1.99$, $p = 0.17$). These results support our hypothesis that synchronization increases as a consequence of task demands specifically between mPFC and task-relevant areas, rather than as a widespread phenomenon.

A second potential confound is related to the characteristics of the connectivity measure used. It has been observed that volume conduction of source activity can affect phase consistency between signals, leading to spuriously increased connectivity estimates (Nolte et al., 2004; Vinck et al., 2011). PLV is notoriously subject to volume conduction artifacts. Therefore, we repeated our analyses using the weighted Phase-Lag Index (wPLI), a measure of phase consistency that disregards connectivity between two signals occurring with a phase lag of 0° , as volume-conducted electric activity is assumed to be recorded by different sensors with negligible time delay. However, the downside of this approach is an increase in the probability of Type II errors, namely reporting no synchronization when true connectivity between signals has close-to-zero phase difference (Vinck et al., 2011).

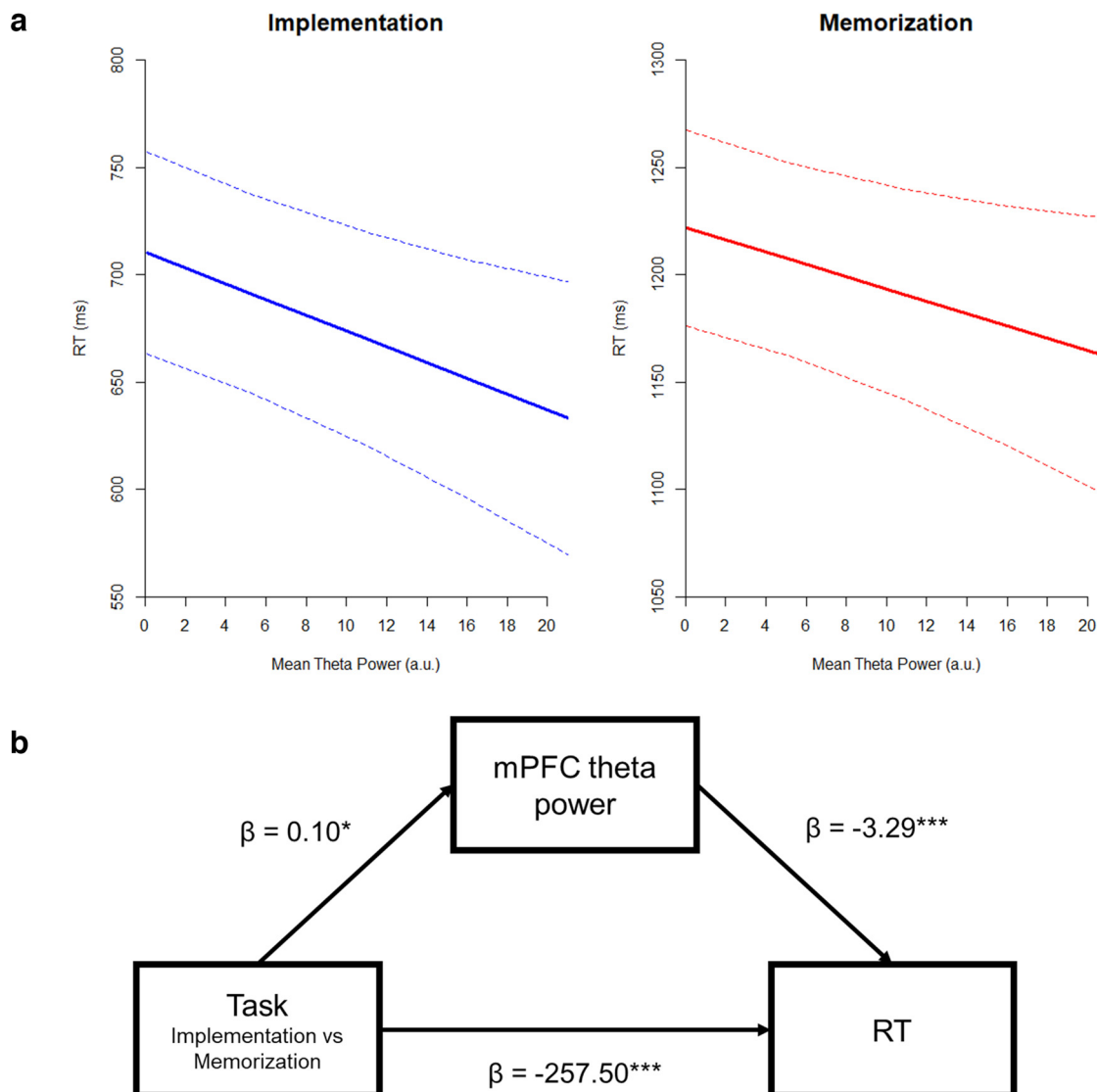


Figure 7. Effect of mean theta power on RTs. **a**, Effect of theta power on RTs, for both Implementation and Memorization. High values of theta power are associated with faster RTs in both tasks. The interaction between theta power and Task was not significant. The dotted lines show the 95% confidence intervals. **b**, Mediation model with beta values. Task significantly influenced mPFC theta power, which in turns affected RTs. Therefore, theta power mediates the effect of tasks demands on behavioral performance. However, the direct effect of Task on RTs remained significant also when accounting for the mediating influence of theta power, suggesting a partial mediation. au: arbitrary units, asterisks denote the significance level (* $p < 0.05$, *** $p < 0.001$).

Overall, wPLI results were consistent with the PLV, albeit less strong for the pair mPFC-Hand ROIs compared with mPFC-LatOcc ROIs ($t_{(0.29)} = 3.04$, $\beta = 0.0007$, CI 95% = $[-0.0001, 0.0015]$, $p = 0.099$; $t_{(0.29)} = 3.63$, $\beta = 0.0014$, CI 95% = $[0.0006, 0.001]$, $p = 0.002$, respectively). We interpreted these findings as confirmatory of the pattern observed with PLV, suggesting larger connectivity estimates for Implementation compared with Memorization.

Discussion

Carrying out novel behaviors on the basis of abstract instructions is a fascinating yet still not fully understood human ability. Despite recent advances in the identification of brain areas involved in this process, and in how these areas

differently encode relevant information (Demagnet et al., 2016; González-García et al., 2017; Palenciano et al., 2019a), how instructed stimuli and responses get flexibly and rapidly combined remains an open question.

A growing body of evidence supports the assumption that the intention to implement the instructed actions triggers a cascade of cognitive processes, ultimately leading to the emergence of a representational state intrinsically different from the initially encoded symbolic content (Muhle-Karbe et al., 2017; González-García et al., 2021). Such reformatting of prioritized items into a behavior-optimized format has been recently proposed as core mechanism to efficiently deal with multiple memoranda and circumvent capacity limitations (Myers et al., 2017). In the context of instructions implementation, we

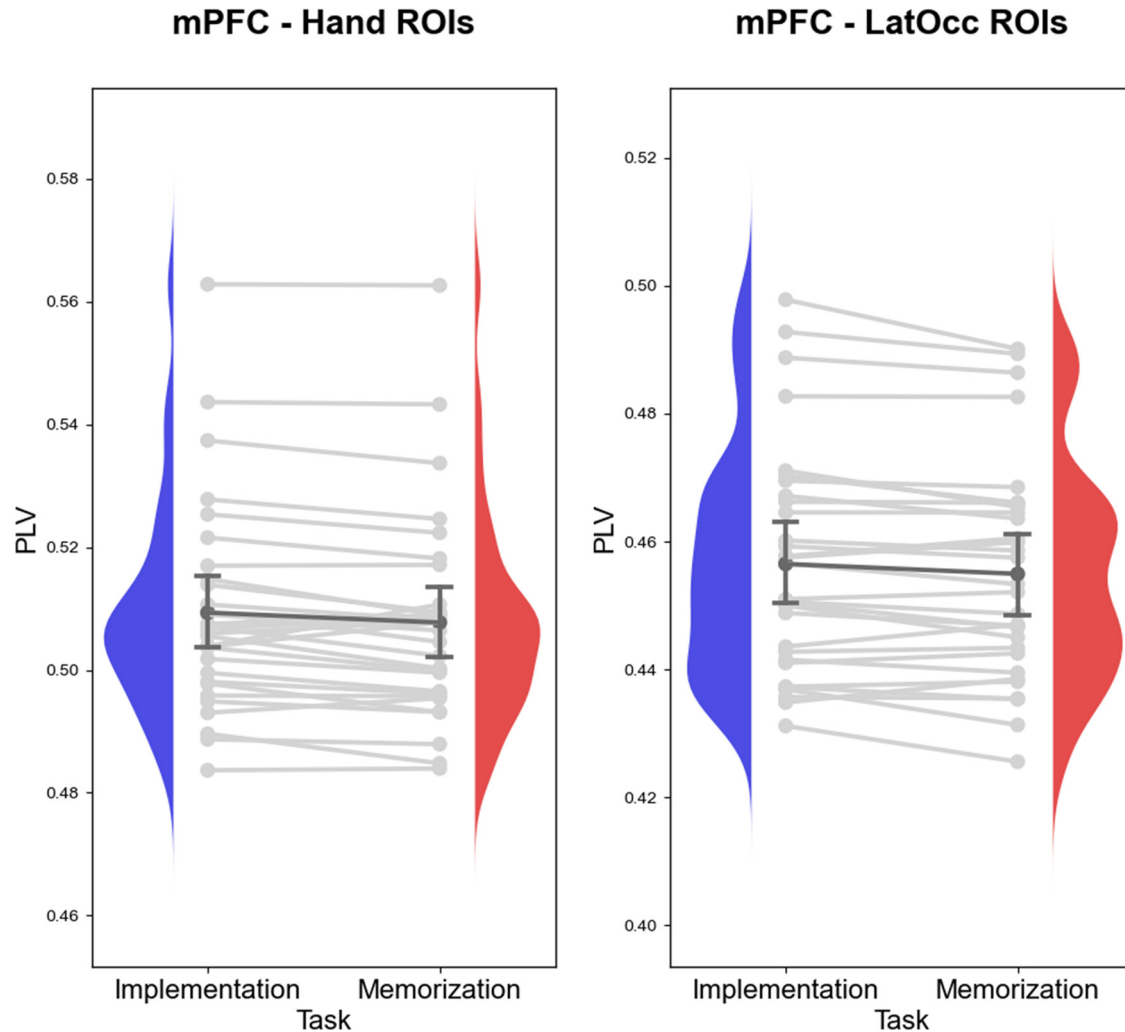


Figure 8. Connectivity between mPFC and posterior ROIs. LMMs revealed that Implementation task demands are associated with stronger connectivity in the theta frequency range between mPFC and motor regions (left panel) and visual regions (right panel). For visualization purposes, the plots depict subject-level averages. Blue and red curves represent the density distributions of subject-level averages of PLV of Implementation and Memorization, respectively. Light gray lines connect the average in the two Tasks for each individual participant, whereas the dark gray line connect the group-level averages (whiskers denote 95% confidence intervals). The same analysis performed on Parahippocampal ROIs as control regions and showing no difference across task demands is reported in Extended Data [Figure 8-1](#). The same analyses performed computing the wPLI and confirming the pattern of results observed with PLV are reported in Extended Data [Figure 8-2](#).

hypothesized that this optimized format consists of strengthened connections between sensory and motor areas representing task-relevant information, coordinated by medial prefrontal structures through long-range phase synchronization. This operationalization is grounded in a body of computational work addressing the role of mPFC theta oscillations in flexibly binding task-relevant areas for upcoming task demands (Verguts, 2017; Verbeke and Verguts, 2019; Verbeke et al., 2020; Senoussi et al., 2022).

In the present study, after replicating at the source level our previous major findings (Formica et al., 2021), we shed light on the interareal dynamics supporting instructions following. We observed strengthened connectivity in the theta frequency range between medial prefrontal and motor/visual areas when novel instructions had to be implemented, as opposed to their simple maintenance. These network

dynamics indicate that proactive proceduralization results in the emergence of a behavior-optimized format relying on flexible patterns of synchronized activity across distant task-relevant brain areas.

Concerning prioritization mechanisms, during both Implementation and Memorization we found a sharp suppression of alpha oscillations in the lateral occipital area contralateral to the attended hemispace. This feature, analogous across task demands, is a hallmark of attentional resources deployment, with the putative function of gating information inflow and contributing to the creation of a functional network (Sauseng et al., 2005; Jensen and Mazaheri, 2010; Mazaheri et al., 2014; Poch et al., 2017; van Ede, 2018; Van Diepen et al., 2019; Keefe and Störmer, 2021). This finding suggests that the two tasks do not differ with respect to resource allocation.

On the contrary, neural signatures of motor preparation were expected to be more prominent during Implementation, given the possibility to activate a specific action plan. We focused on beta dynamics in the motor cortex (Pfurtscheller and Neuper, 1997; Cheyne, 2013; Schneider et al., 2017) and found in both tasks a sustained suppression of beta oscillations contralateral to the instructed response hand, indicating the lateralization of motor preparation. Notably, and contrary to our hypothesis, this suppression was not task-specific, and only marginally larger in Implementation. Although unexpected, this finding might be highlighting the recruitment of motor areas also for the declarative maintenance of SRs that will never have to be overtly executed, supporting the idea of distributed and content-specific maintenance substrates in WM (Christophel et al., 2017).

A second crucial oscillatory feature associated with the proactive preparation for SRs implementation is an increase in midfrontal theta power (Formica et al., 2021). This has been identified as a spectral signature shared across a plethora of mechanisms involved in adaptive control (Cavanagh and Frank, 2014; Cavanagh and Shackman, 2015). Accordingly, in the current study we identified a neural generator for theta oscillations in the mPFC (De La Vega et al., 2016), showing significantly larger activation during Implementation compared with Memorization. Importantly, with our current results we also highlighted the specific functional relevance of this neural activity. Linear models revealed how theta power mediates the effect of different task demands on behavioral performance (Bridwell et al., 2018), providing evidence for the direct implication of mPFC in the implementation of novel instructions.

Stemming from this literature, mPFC has been attributed a central role in determining and instantiating control policies in several computational models of proactive and reactive cognitive control (Dosenbach et al., 2008; Botvinick and Cohen, 2014; Shenhav et al., 2017; Verguts, 2017; Holroyd and Verguts, 2021). In particular, in the work of Verguts and colleagues, mPFC theta oscillations signal the need for adjustments to reach the current goal (Verguts, 2017; Verbeke and Verguts, 2019; Verbeke et al., 2020; Senoussi et al., 2022), and achieve them by synchronizing the activity of task-relevant pairs of sensory and action units, thereby allowing them to communicate more efficiently (Fries, 2005, 2015). Therefore, these models identify in the mPFC the structure responsible to coordinate and operationalize the flexible binding of lower-level modules to meet task demands.

Our theta phase connectivity hypotheses are embedded within this framework, insofar implementation task demands are thought to require the coordination of sensory and motor information in a coherent action-oriented representation. In line with our predictions, we found that theta oscillations between mPFC and motor/visual areas were significantly more synchronized in the Implementation task. Crucially, these findings show that proceduralization triggers the formation of a functional network encompassing frontal and posterior areas through synchronization, compatibly with a view of mPFC exerting top-down control toward posterior areas in response to the specific task demands.

Notably, contrary to our hypotheses, motor/visual areas contralateral and ipsilateral to the hand and hemispace currently relevant showed no difference in their degree of connectivity to the mPFC. This finding is open to alternative explanations. First, it might suggest that top-down synchronization is exerted similarly toward both hemispheres independently of lateralization of stimuli and responses. This interpretation is consistent with a previous study testing the model prediction in a reversal rule learning task involving lateralized responses and reporting bilateral clusters of connectivity between FCz and posterior electrodes (Verbeke et al., 2020). Information on which networks are task-relevant and which should be inhibited could be coded in other aspects of the interactive dynamics between mPFC and posterior areas, such as phase coding or cross-frequency coupling (Helfrich and Knight, 2016), or by means of activity-silent and less resource consuming neurophysiological mechanisms (Stokes, 2015; Masse et al., 2019).

Alternatively, the lack of a significant lateralization effect might be attributed to the selected spatial and temporal features. It cannot be ruled out, for instance, that a short-lasting lateralization in the connectivity patterns emerges only late during the CTI. However, this explanation appears unlikely given the early-onset suppression of beta oscillations in the motor cortex contralateral to the selected response hand, indicating that information on the specific effector is already present shortly after the retro-cue. Moreover, although the selected ROIs were suited to detect the hypothesized lateralized local changes in oscillatory activity, it is possible that lateralization in connectivity with the mPFC is implemented at different stages of the processing hierarchy. Connectivity between mPFC and premotor, rather than motor, cortices might carry information on the currently relevant response hand, and, in a similar fashion, areas at later stages of the visual stream might be more synchronized depending on the stimulus material. In this regard, recent fMRI evidence showed connectivity between the anterior cingulate cortex and visual areas specific for the processing of faces and houses, scaling with task difficulty (Aben et al., 2020). This finding hints at the need for a more fine-grained ROIs definition, and further research should investigate this issue for instance by using independent functional localizers (Baldauf and Desimone, 2014; Kok et al., 2017; Senoussi et al., 2020; González-García et al., 2021).

In the model of flexible binding, the end point is the synchronization of the posterior brain areas coding for the currently relevant stimulus and response. This would be implemented in the gamma frequency range, with the bursts aligning the phase of gamma oscillations (Verguts, 2017). Such synchronization between processing units is difficult to test in the present dataset, as high frequencies (>30 Hz) are significantly more difficult to investigate with EEG (Nottage and Horder, 2015). Although not directly testing for the synchronization between motor and visual areas, we provide evidence that implementation task demands elicit the emergence of a strengthened network of task-relevant brain areas coordinated by the mPFC and instantiated by means of theta-phase synchronization.

Importantly, while theta oscillations from the mPFC provide an explanation on how posterior areas achieve synchronization, the information on which regions should become synchronized is thought to be coded in the lateral PFC (Verguts, 2017). This is consistent with fMRI literature, showing lateral PFC to be a pivotal region in task-set coding (Duncan, 2001; Woolgar et al., 2011; Shahnazian et al., 2022) and dissociating between maintenance and execution task demands (Demanet et al., 2016; González-García et al., 2017, 2021; Palenciano et al., 2019a,b). Previous electrophysiological findings on primates suggest that lateral PFC, and a broader fronto-parietal network, might be encoding task-relevant rule information in the beta range (Buschman et al., 2012; Antzoulatos and Miller, 2016). However, here we put forward and tested hypotheses on theta activity in the mPFC, as these were clearly derivable from the literature and the described model, while remaining agnostic to the role of the lateral PFC. Further research should clarify the oscillatory phenomena associated with instructions following in the lateral PFC with more tailored designs, contributing to integrate the results from the two techniques.

In summary, we focused on the role of mPFC theta oscillations as core mechanism to coordinate the communication between brain areas relevant to execute the instructed behavior. We showed that proactively preparing to implement novel SRs elicits larger theta oscillations in the mPFC, which mediate the effect of task demands on behavioral performance. Crucially, theta-phase synchronization increases between frontal control areas and motor/visual areas, indicating that a procedural, action-oriented format relies on the interplay of distant brain regions.

References

- Aben B, Calderon CB, van den Bussche E, Verguts T (2020) Cognitive effort modulates connectivity between dorsal anterior cingulate cortex and task-relevant cortical areas. *J Neurosci* 40:3838–3848.
- Antzoulatos EG, Miller EK (2016) Synchronous beta rhythms of frontoparietal networks support only behaviorally relevant representations. *Elife* 5:e17822.
- Baldauf D, Desimone R (2014) Neural mechanisms of object-based attention. *Science* 344:424–427.
- Baron RM, Kenny DA (1986) The moderator-mediator variable distinction in social psychological research. Conceptual, strategic, and statistical considerations. *J Person Soc Psychol* 51:1173–1182.
- Bates D, Mächler M, Bolker BM, Walker SC (2014) Fitting linear mixed-effects models using lme4. *J Stat Softw* 67:1–48.
- Bhandari A, Duncan J (2014) Goal neglect and knowledge chunking in the construction of novel behaviour. *Cognition* 130:11–30.
- Bonnefond M, Jensen O (2012) Alpha oscillations serve to protect working memory maintenance against anticipated distracters. *Curr Biol* 22:1969–1974.
- Bonnefond M, Kastner S, Jensen O (2017) Communication between brain areas based on nested oscillations. *eNeuro* 4:ENEURO.0153-16.2017.
- Botvinick MM, Cohen JD (2014) The computational and neural basis of cognitive control: charted territory and new frontiers. *Cogn Sci* 38:1249–1285.
- Bourguignon NJ, Braem S, Hartstra E, De Houwer J, Brass M (2018) Encoding of novel verbal instructions for prospective action in the lateral prefrontal cortex: evidence from univariate and multivariate functional magnetic resonance imaging analysis. *J Cogn Neurosci* 30:1170–1184.
- Brady TF, Konkle T, Alvarez GA, Oliva A (2013) Real-world objects are not represented as bound units: independent forgetting of different object details from visual memory. *J Exp Psychol Gen* 142:791–808.
- Brass M, Liefvooghe B, Braem S, De Houwer J (2017) Following new task instructions: evidence for a dissociation between knowing and doing. *Neurosci Biobehav Rev* 81:16–28.
- Bridwell DA, Cavanagh JF, Collins AGE, Nunez MD, Srinivasan R, Stober S, Calhoun VD (2018) Moving beyond ERP components: a selective review of approaches to integrate EEG and behavior. *Front Hum Neurosci* 12:106–117.
- Brodeur MB, Guérard K, Bouras M (2014) Bank of standardized stimuli (BOSS) phase II: 930 new normative photos. *PLoS One* 9:e106953.
- Bruña R, Pereda E (2021) Multivariate extension of phase synchronization improves the estimation of region-to-region source space functional connectivity. *Brain Multiphysics* 2:100021.
- Bruña R, Maestú F, Pereda E (2018) Phase locking value revisited: teaching new tricks to an old dog. *J Neural Eng* 15:e056011.
- Buschman TJ, Denovellis EL, Diogo C, Bullock D, Miller EK (2012) Synchronous oscillatory neural ensembles for rules in the prefrontal cortex. *Neuron* 76:838–846.
- Cavanagh JF, Frank MJ (2014) Frontal theta as a mechanism for cognitive control. *Trends Cogn Sci* 18:414–421.
- Cavanagh JF, Shackman AJ (2015) Frontal midline theta reflects anxiety and cognitive control: meta-analytic evidence. *J Physiol Paris* 109:3–15.
- Cheyne DO (2013) MEG studies of sensorimotor rhythms: a review. *Exp Neurol* 245:27–39.
- Christophel TB, Klink PC, Spitzer B, Roelfsema PR, Haynes JD (2017) The distributed nature of working memory. *Trends Cogn Sci* 21:111–124.
- Cohen MX (2014) Analyzing neural time series data: theory and practice. Cambridge: MIT Press.
- Cohen MX, Donner TH (2013) Midfrontal conflict-related theta-band power reflects neural oscillations that predict behavior. *J Neurophysiol* 110:2752–2763.
- Cole MW, Laurent P, Stocco A (2013) Rapid instructed task learning: a new window into the human brain's unique capacity for flexible cognitive control. *Cogn Affect Behav Neurosci* 13:1–22.
- Dale AM, Liu AK, Fischl BR, Buckner RL, Belliveau JW, Lewine JD, Halgren E (2000) Dynamic statistical parametric mapping: combining fMRI and MEG for high-resolution imaging of cortical activity. *Neuron* 26:55–67.
- De La Vega A, Chang LJ, Banich MT, Wager TD, Yarkoni T (2016) Large-scale meta-analysis of human medial frontal cortex reveals tripartite functional organization. *J Neurosci* 36:6553–6562.
- Demanet J, Liefvooghe B, Hartstra E, Wenke D, De Houwer J, Brass M (2016) There is more into 'doing' than 'knowing': the function of the right inferior frontal sulcus is specific for implementing versus memorising verbal instructions. *Neuroimage* 141:350–356.
- Desikan RS, Ségonne F, Fischl B, Quinn BT, Dickerson BC, Blacker D, Buckner RL, Dale AM, Maguire RP, Hyman BT, Albert MS, Killiany RJ (2006) An automated labeling system for subdividing the human cerebral cortex on MRI scans into gyral based regions of interest. *Neuroimage* 31:968–980.
- de Vries IEJ, van Driel J, Karacaoglu M, Olivers CNL (2018) Priority switches in visual working memory are supported by frontal delta and posterior alpha interactions. *Cereb Cortex* 28:4090–4104.
- Dosenbach NUF, Fair DA, Cohen AL, Schlaggar BL, Petersen SE (2008) A dual-networks architecture of top-down control. *Trends Cogn Sci* 12:99–105.
- Duncan J (2001) An adaptive coding model of neural function in prefrontal cortex. *Nat Rev Neurosci* 2:820–829.
- Duncan J, Emslie H, Williams P, Johnson R, Freer C (1996) Intelligence and the frontal lobe: the organization of goal-directed behavior. *Cogn Psychol* 30:257–303.

- Formica S, González-García C, Brass M (2020) The effects of declaratively maintaining and proactively proceduralizing novel stimulus-response mappings. *Cognition* 201:104295.
- Formica S, González-García C, Senoussi M, Brass M (2021) Neural oscillations track the maintenance and proceduralization of novel instructions. *Neuroimage* 232:117870.
- Fries P (2005) A mechanism for cognitive dynamics: neuronal communication through neuronal coherence. *Trends Cogn Sci* 9:474–480.
- Fries P (2015) Rhythms for cognition: communication through coherence. *Neuron* 88:220–235.
- González-García C, Arco JE, Palenciano AF, Ramírez J, Ruz M (2017) Encoding, preparation and implementation of novel complex verbal instructions. *Neuroimage* 148:264–273.
- González-García C, Formica S, Liefoghe B, Brass M (2020) Attentional prioritization reconfigures novel instructions into action-oriented task sets. *Cognition* 194:104059.
- González-García C, Formica S, Wisniewski D, Brass M (2021) Frontoparietal action-oriented codes support novel instruction implementation. *Neuroimage* 226:117608.
- Gould IC, Rushworth MF, Nobre AC (2011) Indexing the graded allocation of visuospatial attention using anticipatory alpha oscillations. *J Neurophysiol* 105:1318–1326.
- Gramfort A, Luessi M, Larson E, Engemann DA, Strohmeier D, Brodbeck C, Goj R, Jas M, Brooks T, Parkkonen L, Hämäläinen M (2013) MEG and EEG data analysis with MNE-Python. *Front Neurosci* 7:267.
- Griffin G, Holub A, Perona P (2007) Caltech-256 object category dataset. Pasadena: California Institute of Technology.
- Groppe DM, Makeig S, Kutas M (2009) Identifying reliable independent components via split-half comparisons. *Neuroimage* 45:1199–1211.
- Helfrich RF, Knight RT (2016) Oscillatory dynamics of prefrontal cognitive control. *Trends Cogn Sci* 20:916–930.
- Holroyd CB, Verguts T (2021) The best laid plans: computational principles of anterior cingulate cortex. *Trends Cogn Sci* 25:316–329.
- Itthipuripat S, Wessel JR, Aron AR (2013) Frontal theta is a signature of successful working memory manipulation. *Exp Brain Res* 224:255–262.
- JASP Team (2019) JASP (version 0.11.1)[computer software]. Available at <https://jasp-stats.org/>.
- Jensen O, Mazaheri A (2010) Shaping functional architecture by oscillatory alpha activity: gating by inhibition. *Front Hum Neurosci* 4:186.
- Keefe JM, Störmer VS (2021) Lateralized alpha activity and slow potential shifts over visual cortex track the time course of both endogenous and exogenous orienting of attention. *Neuroimage* 225:117495.
- Klem GH, Lüders HO, Jasper HH, Elger C (1999) The ten-twenty electrode system of the International Federation. *The International Federation of Clinical Neurophysiology. Electroencephalogr Clin Neurophysiol Suppl* 52:3–6.
- Kok P, Mostert P, De Lange FP (2017) Prior expectations induce prestimulus sensory templates. *Proc Natl Acad Sci USA* 114:10473–10478.
- Konkle T, Brady TF, Alvarez GA, Oliva A (2010) Conceptual distinctiveness supports detailed visual long-term memory for real-world objects. *J Exp Psychol Gen* 139:558–578.
- Lachaux JP, Rodriguez E, Martinerie J, Varela FJ (1999) Measuring phase synchrony in brain signals. *Hum Brain Mapp* 8:194–208.
- Liefoghe B, Wenke D, De Houwer J (2012) Instruction-based task-rule congruency effects. *J Exp Psychol Learn Mem Cogn* 38:1325–1335.
- Luke SG (2017) Evaluating significance in linear mixed-effects models in R. *Behav Res* 49:1494–1502.
- Maris E, Oostenveld R (2007) Nonparametric statistical testing of EEG- and MEG-data. *J Neurosci Methods* 164:177–190.
- Masse NY, Yang GR, Song HF, Wang XJ, Freedman DJ (2019) Circuit mechanisms for the maintenance and manipulation of information in working memory. *Nat Neurosci* 22:1159–1167.
- Matuschek H, Kliegl R, Vasishth S, Baayen H, Bates D (2017) Balancing type I error and power in linear mixed models. *J Mem Lang* 94:305–315.
- Mazaheri A, van Schouwenburg MR, Dimitrijevic A, Denys D, Cools R, Jensen O (2014) Region-specific modulations in oscillatory alpha activity serve to facilitate processing in the visual and auditory modalities. *Neuroimage* 87:356–362.
- McLelland D, VanRullen R (2016) Theta-gamma coding meets communication-through-coherence: neuronal oscillatory multiplexing theories reconciled. *PLoS Comput Biol* 12:e1005162.
- Miller EK, Cohen JD (2001) An integrative theory of prefrontal cortex function. *Annu Rev Neurosci* 24:167–202.
- Milner B (1963) Effects of different brain lesions on card sorting: the role of the frontal lobes. *Arch Neurol* 9:90–100.
- Mok RM, Myers NE, Wallis G, Nobre AC (2016) Behavioral and neural markers of flexible attention over working memory in aging. *Cereb Cortex* 26:1831–1842.
- Mormann F, Lehnertz K, David P, Elger CE (2000) Mean phase coherence as a measure for phase synchronization and its application to the EEG of epilepsy patients. *Physica D* 144:358–369.
- Muhle-Karbe PS, Duncan J, De Baene W, Mitchell DJ, Brass M (2017) Neural coding for instruction-based task sets in human frontoparietal and visual cortex. *Cereb Cortex* 27:1891–1905.
- Myers NE, Walther L, Wallis G, Stokes MG, Nobre AC (2015) Temporal dynamics of attention during encoding versus maintenance of working memory: complementary views from event-related potentials and alpha-band oscillations. *J Cogn Neurosci* 27:492–508.
- Myers NE, Stokes MG, Nobre AC (2017) Prioritizing information during working memory: beyond sustained internal attention. *Trends Cogn Sci* 21:449–461.
- Nieuwenhuis S, Forstmann BU, Wagenmakers EJ (2011) Erroneous analyses of interactions in neuroscience: a problem of significance. *Nat Neurosci* 14:1105–1107.
- Nolte G, Bai O, Wheaton L, Mari Z, Vorbach S, Hallett M (2004) Identifying true brain interaction from EEG data using the imaginary part of coherency. *Clin Neurophysiol* 115:2292–2307.
- Nottage JF, Horder J (2015) State-of-the-art analysis of high-frequency (gamma range) electroencephalography in humans. *Neuropsychobiology* 72:219–228.
- Onton J, Delorme A, Makeig S (2005) Frontal midline EEG dynamics during working memory. *Neuroimage* 27:341–356.
- Palenciano AF, González-García C, Arco JE, Pessoa L, Ruz M (2019a) Representational organization of novel task sets during proactive encoding. *J Neurosci* 39:8386–8397.
- Palenciano AF, González-García C, Arco JE, Ruz M (2019b) Transient and sustained control mechanisms supporting novel instructed behavior. *Cereb Cortex* 29:3948–3960.
- Peirce JW (2007) PsychoPy-psychophysics software in Python. *J Neurosci Methods* 162:8–13.
- Perrin F, Pernier J, Bertrand O, Echallier JF (1989) Spherical splines for scalp potential and current density mapping. *Electroencephalogr Clin Neurophysiol* 72:184–187.
- Pfurtscheller G, Neuper C (1997) Motor imagery activates primary sensorimotor area in humans. *Neurosci Lett* 239:65–68.
- Poch C, Capilla A, Hinojosa JA, Campo P (2017) Selection within working memory based on a color retro-cue modulates alpha oscillations. *Neuropsychologia* 106:133–137.
- Riddle J, Scimeca JM, Cellier D, Dhanani S, Esposito MD, Riddle J, Scimeca JM, Cellier D, Dhanani S, Esposito MD (2020a) Causal evidence for a role of theta and alpha oscillations in the control of working memory. *Curr Biol* 30:1748–1747.
- Riddle J, Vogelsang DA, Hwang K, Cellier D, D'Esposito M (2020b) Distinct oscillatory dynamics underlie different components of hierarchical cognitive control. *J Neurosci* 40:4945–4953.
- Ruge H, Wolfensteller U (2010) Rapid formation of pragmatic rule representations in the human brain during instruction-based learning. *Cereb Cortex* 20:1656–1667.

- Sassenhagen J, Draschkow D (2019) Cluster-based permutation tests of MEG/EEG data do not establish significance of effect latency or location. *Psychophysiology* 56:e13335.
- Sauseng P, Klimesch W (2008) What does phase information of oscillatory brain activity tell us about cognitive processes? *Neurosci Biobehav Rev* 32:1001–1013.
- Sauseng P, Klimesch W, Stadler W, Schabus M, Doppelmayr M, Hanslmayr S, Gruber WR, Birbaumer N (2005) A shift of visual spatial attention is selectively associated with human EEG alpha activity. *Eur J Neurosci* 22:2917–2926.
- Sauseng P, Griesmayr B, Freunberger R, Klimesch W (2010) Control mechanisms in working memory: a possible function of EEG theta oscillations. *Neurosci Biobehav Rev* 34:1015–1022.
- Schneider D, Barth A, Wascher E (2017) On the contribution of motor planning to the retroactive cuing benefit in working memory: evidence by mu and beta oscillatory activity in the EEG. *Neuroimage* 162:73–85.
- Senoussi M, Vanrullen R, Reddy L (2020) Anticipatory reinstatement of expected perceptual events during visual sequence learning. *BioRxiv*. doi:10.1101/2020.11.28.402123.
- Senoussi M, Verbeke P, Desender K, De Loof E, Talsma D, Verguts T (2022) Theta oscillations shift towards optimal frequency for cognitive control. *Nat Hum Behav* 6:1000–1013.
- Shahnazian D, Senoussi M, Krebs RM, Verguts T, Holroyd CB (2022) Neural representations of task context and temporal order during action sequence execution. *Top Cogn Sci* 14:223–218.
- Shenhav A, Musslick S, Lieder F, Kool W, Griffiths TL, Cohen JD, Botvinick MM (2017) Toward a rational and mechanistic account of mental effort. *Annu Rev Neurosci* 40:99–124.
- Souza AS, Oberauer K (2016) In search of the focus of attention in working memory: 13 years of the retro-cue effect. *Atten Percept Psychophys* 78:1839–1860.
- Stokes MG (2015) “Activity-silent” working memory in prefrontal cortex: a dynamic coding framework. *Trends Cogn Sci* 19:394–405.
- Tingley D, Yamamoto T, Hirose K, Keele L, Imai K (2014) Mediation: R package for causal mediation analysis. *J Stat Soft* 59:1–38.
- Van Diepen R, Foxe JJ, Mazaheri A (2019) The functional role of alpha-band activity in attentional processing: the current zeitgeist and future outlook. *Curr Opin Psychol* 29:229–238.
- van Ede F (2018) Mnemonic and attentional roles for states of attenuated alpha oscillations in perceptual working memory: a review. *Eur J Neurosci* 48:2509–2507.
- van Ede F, Chekroud SR, Stokes MG, Nobre AC (2019) Concurrent visual and motor selection during visual working memory guided action. *Nat Neurosci* 22:477–483.
- Verbeke P, Verguts T (2019) Learning to synchronize: how biological agents can couple neural task modules for dealing with the stability-plasticity dilemma. *PLoS Comput Biol* 15:e1006604.
- Verbeke P, Ergo K, De Loof E, Verguts T (2020) Learning to synchronize: midfrontal theta dynamics during rule switching. *J Neurosci* 41:1516–1528.
- Verguts T (2017) Binding by random bursts: a computational model of cognitive control. *J Cogn Neurosci* 29:1103–1118.
- Vinck M, Oostenveld R, Van Wingerden M, Battaglia F, Pennartz CMA (2011) An improved index of phase-synchronization for electrophysiological data in the presence of volume-conduction, noise and sample-size bias. *Neuroimage* 55:1548–1565.
- Voloh B, Womelsdorf T (2016) A role of phase-resetting in coordinating large scale neural networks during attention and goal-directed behavior. *Front Syst Neurosci* 10:18.
- Woolgar A, Hampshire A, Thompson R, Duncan J (2011) Adaptive coding of task-relevant information in human frontoparietal cortex. *J Neurosci* 31:14592–14599.
- Zhao M, Marino M, Samogin J, Swinnen SP, Mantini D (2019) Hand, foot and lip representations in primary sensorimotor cortex: a high-density electroencephalography study. *Sci Rep* 9:1–12.